

ENERGY SPECTRA OF ELEMENTS WITH $18 \leq Z \leq 28$
BETWEEN 10 AND 300 GeV/amu

Michael D. Jones^a, J. Klarmann^a, E. C. Stone^b, C. J. Waddington^c, W. R. Binns^a,
T. L. Garrard^b, M. H. Israel^a

a) Washington University, St. Louis, MO 63130, USA

b) California Institute of Technology, Pasadena, CA 91125 USA

c) University of Minnesota, Minneapolis, MN 55455, USA

1. Introduction. The HEAO-3 Heavy Nuclei Experiment (Binns, *et al.*, 1981) is composed of ionization chambers above and below a plastic Cherenkov counter. We have measured the energy dependence of the abundances of elements with atomic number, Z , between 18 and 28 at very high energies where they are rare and thus need the large area \times time of this experiment. We extend the measurements of the Danish-French HEAO-3 experiment (Englemann, *et al.*, 1983) to higher energies, using the relativistic rise of ionization signal as a measure of energy, and determine source abundances for Ar and Ca.

2. Data Analysis. We confine this analysis to events in the $1.1 \text{ m}^2 \text{sr}$ in which the cosmic rays penetrate all six ionization chambers, and to the first 370 days of the flight, when all six ionization chambers were functioning properly. These selections give the highest possible ionization resolution. We select only events incident with geomagnetic cutoff greater than 8 GV, so Z is determined by the Cherenkov signal. We further require agreement between the means of the three ionization chamber signals above the Cherenkov and those below, to eliminate most nuclear interactions inside the instrument.

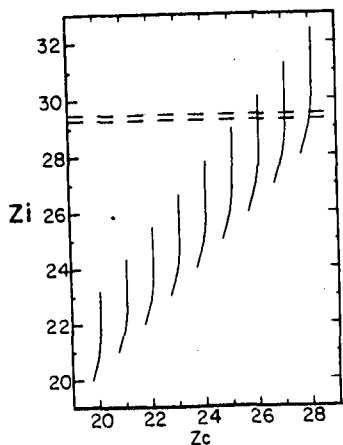


Figure 1

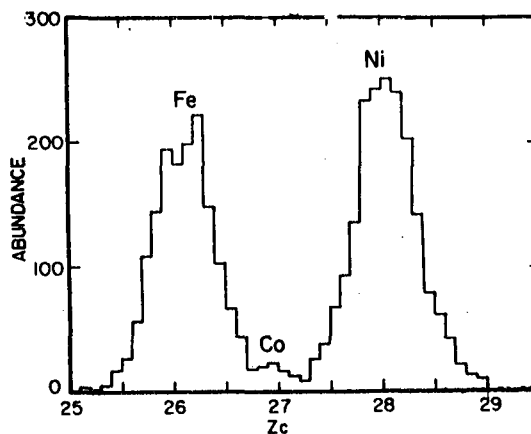


Figure 2

Figure 1 is a schematic plot showing the locus of events for each element, $20 \leq Z \leq 28$. Z_c is the square-root of the Cherenkov signal normalized so $Z_c \approx Z$ at high energy. Z_i is the square-root of the ionization normalized so $Z_i = Z$ at minimum-ionizing. Figure 2 is a histogram of Z_c for events with $29.3 < Z_i < 29.5$, the region between the dashed lines in figure 1. This histogram includes Fe, Co, and Ni at about 130, 34, and 12 GeV/amu respectively. The abundance of each element in each of eighty such histograms is determined by maximum-likelihood fitting.

Corrections to these raw abundances were calculated to account for interactions both in the lid in front of the first ionization chamber and in the Cherenkov counter and other material between the ionization chambers. The latter calculation included only charge changes of one or two charge units, other interactions having been eliminated by the requirement for agreement between upper and lower ionization chambers. The calculation assumed that at all energies the total cross-sections were given by the formula of Westfall *et al.* (1979) and the partial cross-sections for changing by n charge units were the same fraction of the total cross-section for any projectile as was measured by Webber and Brautigam (1982) at 980 MeV/amu for Fe on C. These calculated corrections lowered the raw abundance ratios by typically 10 to 30 percent.

3. Energy Scale. We used Z_i/Z as a measure of energy, and derived an empirical energy calibration by comparing our Fe observations with an Fe energy spectrum derived from a compilation of previously published measurements (Webber, 1982). This Fe spectrum was multiplied by an empirical geomagnetic transmission function which represented the fraction of time when the geomagnetic cutoff permitted Fe of that energy to reach the instrument; the product was the effective Fe spectrum at the instrument, averaged over many orbits. This energy spectrum was then converted to a Z_i/Z spectrum using a trial form of the energy dependence of Z_i/Z . Finally this calculated spectrum was folded with the instrument's ionization resolution, and the resulting Z_i/Z spectrum was compared with the data. The process was iterated, by changing the assumed form of the energy dependence of Z_i/Z , until the calculated and observed spectra of Fe agreed.

The resulting energy dependence is consistent, between about 10 and 100 GeV/amu, with one derived independently for a different detector system by Barthelmy *et al.* (1985, OG 4.1-7). Above about 200 GeV/amu, the shape of our calibration curve depends upon the assumption we made that the Fe energy spectrum falls as a power-law with exponent -2.7 at energies above those where it has been measured.

Abundance ratios derived from data in a particular Z_i/Z histogram were plotted at the mean energy from which those particles came, assuming the Fe energy spectrum and the calibration curve described above. The energy resolution implied by our ionization resolution of 0.40 charge units is comparable to the spacing of the points in figure 3.

4. Results. Figure 3 gives the resulting abundances of several elements relative to Fe as a function of energy. The X symbols are the results of the DF experiment (Englemann, 1983), while the O symbols are the results of this experiment. In every case our results are consistent with those of the DF experiment in the interval where both experiments apply, 10 to 25 GeV/amu. At higher energies our data generally continue the DF trend.

Our data above 10 GeV/amu suggest a Ni/Fe ratio slightly dependent upon energy, with a best fit power law of exponent -0.050 ± 0.016 . If we ignore this slight variation with energy, then the mean value of the Ni/Fe ratio over our data is 0.054 ± 0.001 .

For the secondary ratios, K/Fe, Sc/Fe, Ti/Fe, and V/Fe, our data indicate an extension to about 100 GeV/amu of the same power law dependence as was indicated by the DF data. Figure 4 shows the best fit exponent for each of these ratios combining the DF and our data. The steepening of the slope with decreasing Z is expected as lower Z elements have greater contributions from tertiary nuclei.

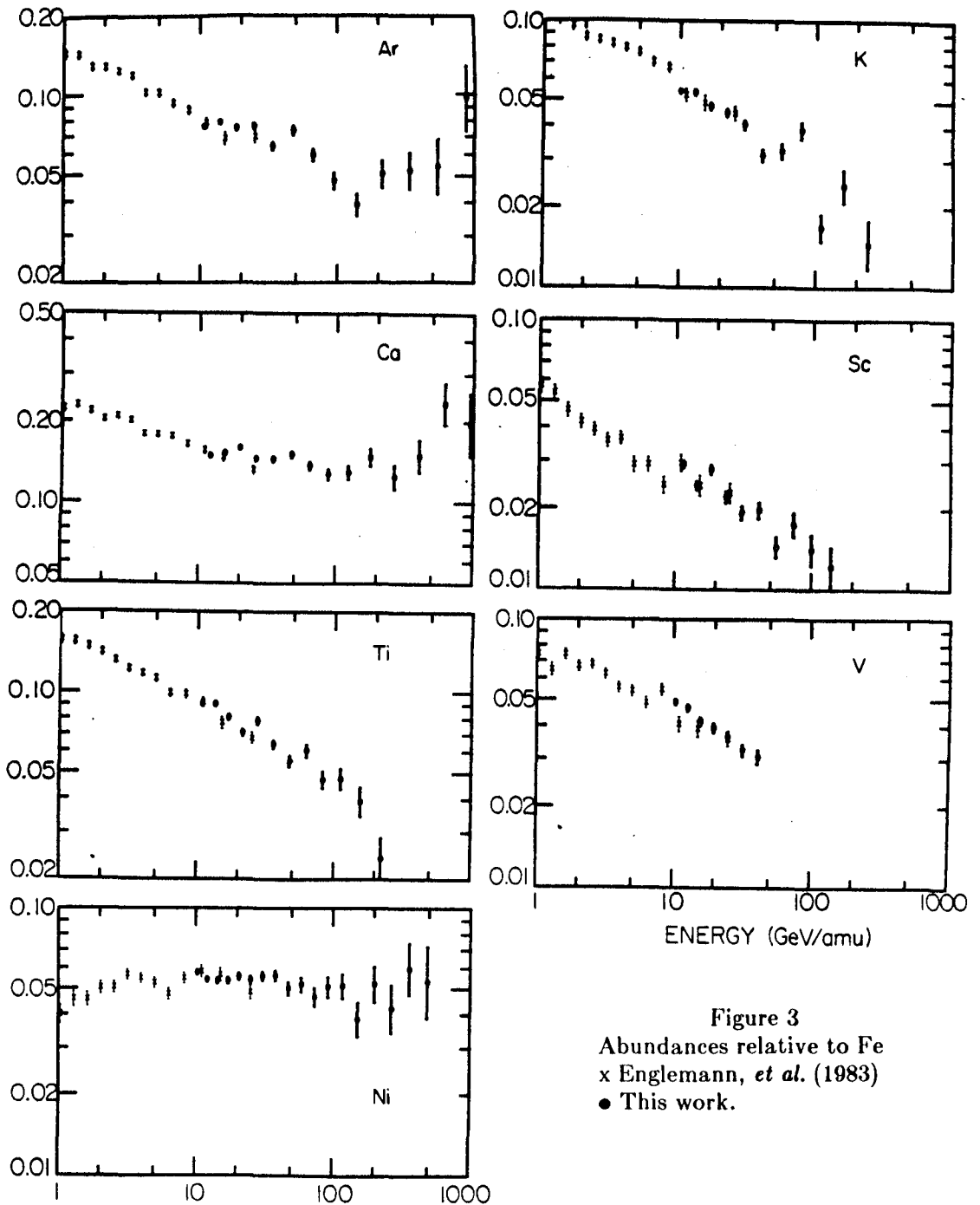


Figure 3
Abundances relative to Fe
x Englemann, *et al.* (1983)
● This work.

Our data indicate a leveling of the Ca/Fe ratio above the energies of the DF experiment, as would be expected from an energy-independent primary component becoming increasingly significant at higher energies as the secondary component becomes less abundant. We fitted the combination of the DF and our ratios to a function $aE^p + b$. With $p = -0.295 \pm 0.010$, interpolated from figure 4, the result is primary Ca/Fe = 0.094 ± 0.004 . A galactic propagation calculation on the DF data (Lund, 1984) gives a source abundance of Ca/Fe = 0.065 ± 0.019 .

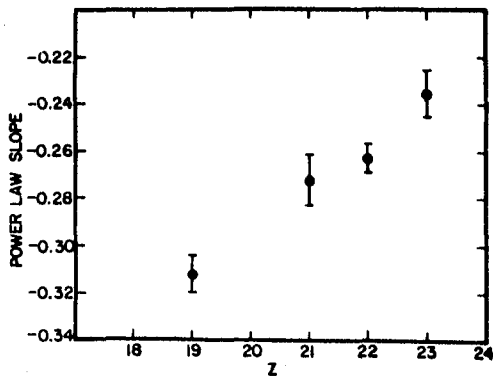


Figure 4
Exponent of power law fit to
abundance of element Z
relative to Fe.

A similar fit to the energy dependence of Ar/Fe, but with $p = -0.33 \pm 0.01$, gives primary Ar/Fe = 0.026 ± 0.003 . Propagation of the DF data (Lund, 1984) gives Ar/Fe = 0.032 ± 0.008 . Source abundances inferred from such galactic propagations on observed abundances 2.5 to 5 times higher must depend critically upon the adopted fragmentation cross-sections, while our extension of observations above 100 GeV/amu permits inference of source abundances without galactic propagation calculations.

5. Acknowledgement. This work was supported in part by NASA grants NAG 8-498, 500, 502, and NGR 05-002-160, 24-005-050, and 26-008-001.

6. References

- Barthelmy, S.D., M.H. Israel, J. Klarmann, 1985, this conference OG4.1-7.
 Binns, W.R., *et al.*, 1981, *Nucl. Instr. Meth.*, 185, 415.
 Englemann, J.J., *et al.*, 1983, *18th ICRC (Bangalore)* 2, 17.
 Lund, N., 1984, *Adv. Space Res.*, 4, (No.2-3), 5.
 Webber, W.R., 1982, *Comp. Origin of Cos. Rays*, ed. M.M.Shapiro, 25.
 Webber, W.R. and D.A. Brautigam, 1982, *Ap. J.*, 260, 894.
 Westfall, G.D., *et al.*, 1979, *Phys. Rev. C*, 19, 1309.